High-Agility, Miniaturized Attitude Control Sensors and Actuators in an All-in-one Module

Article *in* Transactions of the Japan Society for Aeronautical and Space Sciences, Aerospace Technology Japan · November 2016

DOI: 10.2322/tastj.14.Pd_47

CITATION
1

READS
123

4 authors, including:

Shinji Mitani
Japan Aerospace Exploration Agency
37 PUBLICATIONS **111** CITATIONS
SEE PROFILE

Shuhei Shigeto
Japan Aerospace Exploration Agency
5 PUBLICATIONS **11** CITATIONS
SEE PROFILE

Takuya Kanzawa
Japan Aerospace Exploration Agency
19 PUBLICATIONS **29** CITATIONS
SEE PROFILE

Trans. JSASS Aerospace Tech. Japan
Vol. 14, No. ists30, pp. Pd_47-Pd_53, 2016

High-Agility, Miniaturized Attitude Control Sensors and Actuators in an All-in-one Module

By Shinji MITANI,[1)] Shuhei SHIGETO,[1)] Takuya KANZAWA[1)] and Koji YAMANAKA[1)]

[1)]*Research and Development Directorate, JAXA, Tsukuba, Japan*

(Received July 31st, 2015)

A three-axis attitude control function module was assembled into a highly integrated cubic package (10^3 cm^3 dimension: 1U-sized). The key feature of the cubic module is its high-agility functionality, which is realized by a novel, compact electromagnetic braking mechanism combined with a ferromagnetic wheel. In this study, the proposed concept is compared with existing 1-axis wheel assemblies and the conventional CMG scheme in terms of momentum storage per mass/volume, maneuvering speed, and compactness. A prototype of the module was manufactured to demonstrate this innovative concept.

Key Words: Attitude Control, Miniaturized ACS Assembly, High-agility Actuator

1. Introduction

When designing a compact package module that employs a three-axis attitude control (AC) function via its sensors, actuators, and processor, it is vitally important to consider both minimizing the cost of the AC subsystem components and space-saving within the satellite. By miniaturizing a three-axis AC function module into a highly integrated package, it is possible to compress the mounting space occupied by the conventional AC constituents into a space using 10^3 cm^3 (1U), allowing for the installation of larger mission payloads. The number of one-module developments and products is gradually increasing[1,2)], and their target customer is primarily CubeSat. Therefore, all AC functions, including the star tracker (ST), gyroscopes, GPS receiver (GPSR), reaction wheels (RWs), magnetic torquers, and the attitude processing computer should ideally be encapsulated into 1U of space. At present, small-type control moment gyroscopes (CMGs) are being developed worldwide[3,4)], and wearable CMGs for variable vector countermeasure suits have been developed for human deep-space activity missions[5)].However, 1U AC packages that also include highly agile actuators such as CMGs, have not yet been constructed.

In this study, an actuator-like CMG functionality is included within a developed 1U package. Its featured high-agility functionality is realized through our proposed compact electromagnetic braking mechanism combined with a ferromagnetic wheel. It is considered that this novel mechanism could replace the large gimbal mechanism used in conventional CMGs to realize maneuvering and high-agility pointing missions. In addition, the developed application is aimed for use in the following: the active movement (jump and hop) of exploration robots along asteroid or lunar surfaces[6-8)]; the 3-axis stabilized module exchangeable with on-orbit satellites; and the additional AC functionality attached to non-corporative on-orbit debris (Fig. 1). Preliminary analysis and selected experimental demonstrations are shown for such applications using the electromagnetic braking mechanism.

At this stage of development, the product concept mainly focuses on high-agility actuator usage to make the best use of the 1U of space as an inertial mass. GPSR and ST are not implemented. To the best of our knowledge, this is the first attempt to package rapid maneuvering functionality into one module as previous attempts were hindered by gimbal mechanism interference. In our study, by considering the problem from a different angle, we are thus able to propose a simple means for suddenly stopping wheel rotation and controlling the momentum of a spacecraft. In addition, we adapt a compact electromagnetic braking mechanism and place the three mechanisms within a 1U-sized package. Furthermore, in this study, the differences between our new approach and the conventional CMG scheme, particularly in maneuver speeds under constant angular momentum, are compared and discussed. Finally, we achieve the development of a high-agility unit named Cubli[9)]; it can jump and balance and is smaller than a 15^3 cm^3 3D inverted pendulum.

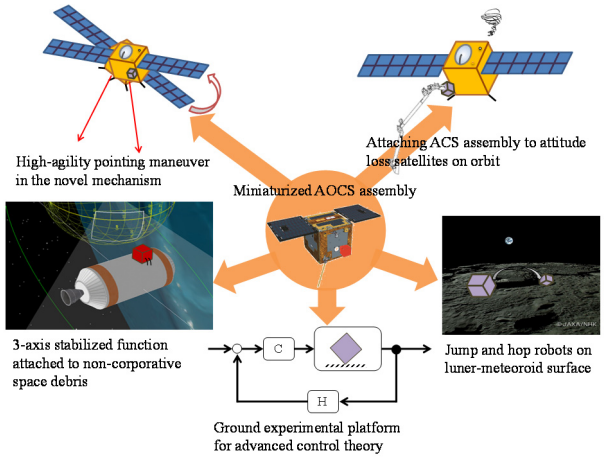

Fig. 1. Potential applications for our proposed miniaturized ACS all-in-one module concept.

2. Benchmark Study

2.1. Momentum storage comparison

The arrangement options of 3-axis wheels are limited when housed within one module. Fig. 2 shows the maximal arrangement for one inertial rotor housed within the side (L) of a cube. For this arrangement, the angular stored momentum for the 1-axis wheel mass and volume are plotted as solid lines in Fig. 3. Stainless steel and tungsten densities are assumed to be equivalent to that of the wheel rotor, and the maximum rotation speed is set to 6000 rpm. In Fig. 3, the specifications of various ready-made 1-axis wheels are plotted as blue circles. A similar study was conducted by Greenbaum et al.[10], where momentum storage h was plotted against mass m, and this appears to indicate a clear threshold for performance. However, there are many wheels that ride along the threshold $h \propto m^{5/3}$, which is presumed from the relationships of $h \propto L^5$ and $m \propto L^3$, and thus momentum storage as a function of unit mass is unlikely to become a key selling point, as it is highly limited by physics. However, this relationship is several times superior when compared with angular momentum per volume. Note that only 3-axis wheels are considered. It is also considered that containing the inertia sensors and attitude processing computer within the same package generates additional benefits, in terms of unit weight and compactness.

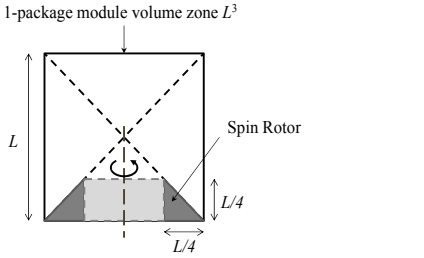

Fig. 2. Maximal arrangement within a one-package module.

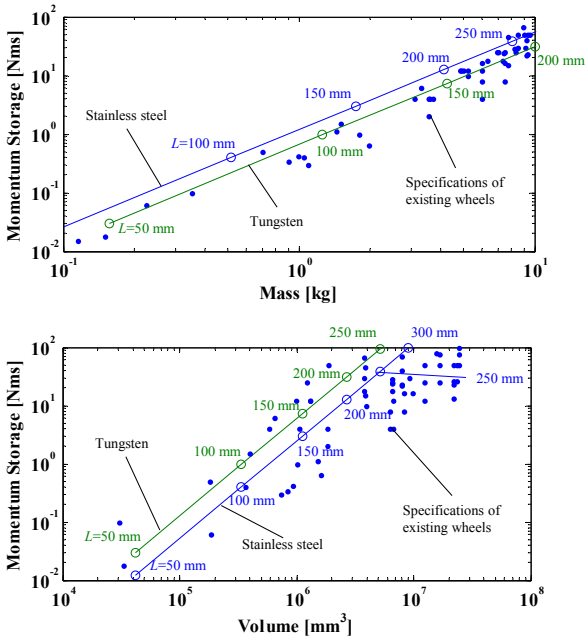

Fig. 3. Momentum storage versus mass (top); momentum storage versus volume (bottom).

2.2. Maneuverability comparison

One of the main merits of our proposed AC module is that the packaging includes both reaction torque functionality and control momentum functionality. Our proposed method for rapidly changing the angular moment uses braking via the solenoid mechanism; the mechanism involved in braking the wheel and the reasons for the component compactness of this method are explained below.

For one-dimensional rotation, placing a reaction wheel with the same inertia in parallel realizes the control moment function, as shown in Fig. 4a. First, the two units of the wheel are arranged coaxially, and they are then rotated at the same speed but in reverse directions. At this point, there is no momentum exchange occurrence between the wheels and the satellite body because the momentums of the two wheels nullify each other. One of the wheels is then stopped at the maneuver starting time and the satellite begins to rotate; when the satellite reaches its target attitude the other wheel is then stopped. In this way, a rest-to-rest attitude maneuver is realized, which does not cause residual rotational speed. Three of the same mechanisms are used in a three-dimensional maneuver, where a two-unit module (which houses three orthogonal wheels) is installed and its co-axial wheels are rotated in opposing directions, as shown in Fig. 4b.

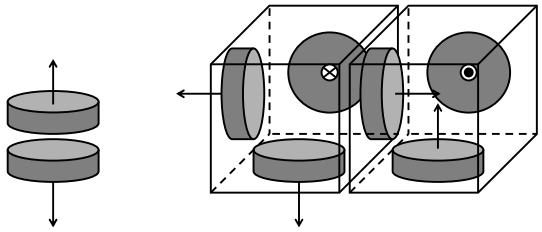

(a) (b)

Fig. 4. a) 1D maneuver configuration with two wheels; b) 3D maneuver configuration with six wheels.

According to the simple angular exchange law, the proposed method gives an interval of time, t_p, which uses the change in the maneuvering angle, $\Delta\theta_s$

$$t_p = \frac{I_s}{h} \cdot \Delta\theta_s \qquad (1),$$

where h is the initially stored momentum of the wheel and I_s is the inertial moment of the satellite. Let us then use this method for an operational case in which one wheel is accelerated and decelerated, generating maximal torque. The 1D rotational equation for one wheel is

$$I_w\dot{\omega}_w = T_m - C_w\omega_w \qquad (2),$$

where I_w is the inertial moment of the wheel, $\omega_w(t)$ is the wheel speed, T_m is the output torque, and C_w is the dynamic friction coefficient of the wheel. When T_m is constant and $\omega_w(0) = 0$, Eq. (2) can be solved as a time, t, function.

$$\omega_w(t) = \frac{T_m}{C_w}\left[1 - \exp\left(-\frac{C_w}{I_w}t\right)\right] \quad (3)$$

Substituting Eq. (3) into the rotational equation for the satellite

$$I_s\dot{\omega}_s = -T_m + C_w\omega_w \quad (4),$$

the attitude angle of satellite $\theta_s(t) \equiv \int_0^t \omega_s(\tau)d\tau$ is then

$$\theta_s(t) = -\frac{1}{2}\cdot\frac{T_m}{I_s}t^2 + O(t^3) \quad (5).$$

For simplification, the order of t^3 can be neglected. The sign of T_m is inverted in the middle of time t_w, which changes θ_s by $\Delta\theta_s$. Provided that $t_w \gg I_w/C_w$, the relation ship between $\Delta\theta_s$ and t_w is

$$\frac{\Delta\theta_s}{2} \sim \frac{1}{2}\cdot\frac{T_m}{I_s}\cdot\left(\frac{t_w}{2}\right)^2 \quad (6).$$

By defining $T_d \equiv C_w h/I_w$, $h \equiv I_w\omega_w^{max} = T_m t_w/2$ and substituting these and Eq. (1) into Eq. (6), then t_w is estimated as

$$t_w \sim \left\|\frac{2T_d}{T_m}\right\|\cdot t_p \quad (7).$$

When comparing steady rotational speeds where there is a balancing of the maximum torque and the dynamic friction torque, $T_m \sim T_d$, then $t_w \sim 2t_p$, which takes twice the time, t_p. Since our proposed method uses two wheels and potentially twice the angular momentum, the result is considered to be reasonable.

In the rule-of-thumb estimation, it is assumed that sufficient torque will occur until the required rotational speed is achieved over a short time; a powerless motor would require a greater maneuvering time. However, using our proposed method, a high-agility maneuver is possible at any time, even with a powerless motor, if the rotational speed is increased prior to the manoeuver. This means that it is possible to prepare for the emergency observation of sudden onsets of gamma-ray bursts[11] or for a pre-planned maneuvering operation. After a manoeuver is completed, it is possible to use a normal reaction wheel at rest speed. When compared with using wheels at high-speed, a large torque can thus be generated immediately after the manoeuver ends. This difference thus affects the attitude attained after the manoeuver.

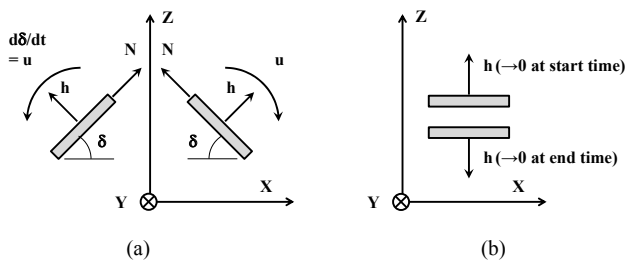

(a) (b)

Fig. 5. a) 2-CMG parallel arrangement, b) our proposed arrangement (with no gimbal mechanism).

Next, let us compare our proposed method with the conventionally-used CMG method. Consider a 2-CMG parallel arrangement, where the gimbal axes are perpendicular to the z–x plane and are parallel to each other, as depicted in Fig. 5a.[3] The dynamics equation is as follows:

$$I_s\dot{\omega}_s = 2uh\sin\delta \quad (8),$$

where h is the CMG-stored momentum, δ is the gimbal angle, and $u \equiv \dot{\delta}$ is the gimbal rate. We then consider the operation of the CMG, wherein the gimbals move symmetrically at a constant rate and then move back to their initial position angle in a scissor-like manner. If u is constant, Eq. (8) is explicitly solved in terms of $\theta_s(t)$.

$$q(ut) \equiv \theta_s(t)/(\frac{h}{I_s u}) = 2[ut - \sin(ut)] \quad (9)$$

provided that the initial gimbal angle is 0. In this, q is defined as the nondimensional quantity of $\theta_s(t)$, and ut is the nondimensional quantity of time t, which is physically equivalent to the gimbal variation angle, δ. We thus discuss the nondimensional values of q and ut. Suppose that when δ reaches $\pi/2$ rad, δ is maintained and the satellite is cruising. The maneuvering angle q^*, in which $\delta = \pi/2$ is achieved, is $\pi - 2$. If the maneuvering angle Δq is larger than $2q^*$, the satellite cruises while holding δ as $\pi/2$, until its return point; this nondimensional interval of time is

$$ut = \frac{\Delta q}{2} + 2, \qquad \Delta q \geq 2q^* \quad (10).$$

In contrast, in the arrangement of our proposed mechanism, after a simple momentum exchange, the nondimensional transformation of Eq. (1) leads to

$$ut = \Delta q \quad (11).$$

When Eqs. (10) and (11) are compared, if Δq is smaller than 4, our proposed arrangement is better than the 2-CMG parallel arrangement. Fig. 6 shows the maneuvering profiles for cases of Δq = 2, 4, and 6. These results are reasonable, in that 2-CMG has an advantage at larger maneuvering angles, since a $2h$ momentum exchange can occur during a longer cruising time. For example, if the parameters $I_s = 10\ \mathrm{kg\,m^2}$, $h = 0.28\ \mathrm{N\,ms}$, and $u = 9^\circ/\mathrm{s}$ are taken from Lappas[3], then our proposed method is superior when the maneuvering angle $\Delta\theta_s$ is less than 40.85°. In addition, if I_s is smaller, the maneuvering using our proposed arrangement is faster.

Table 1 summarizes the trade-off seen in the results, where the time-consuming 2-CMG method is described in the case of $\Delta\theta_s > 2q^*h/I_s u$ (the bracketed number represents the 3D arrangement). It can be seen that the conventional CMG method requires four wheels, whereas our proposed method requires six wheels. However, the advantage of our method is that the servo mechanism and wheel-maneuvering volumes are reduced.

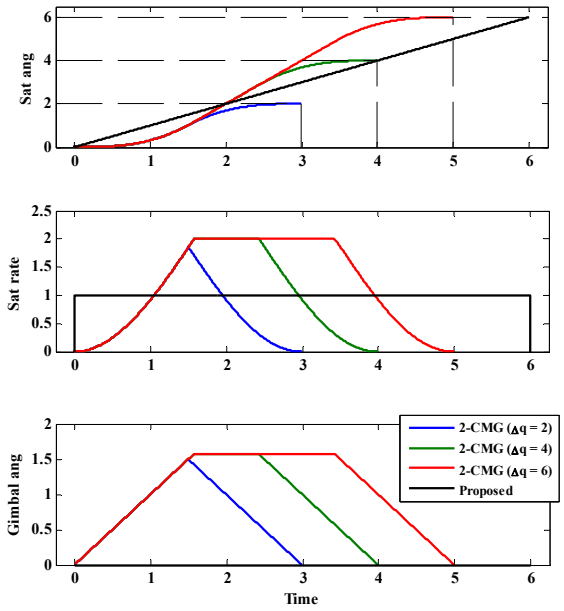

Fig. 6. Comparison between the 2-CMG method and our proposed method: satellite maneuver angle (top), satellite rate (middle), and gimbal angle (bottom). Note that our proposed method has no gimbal mechanism.

Table 1. Comparison of arrays and maneuvering time.

	RW	CMG	Proposition
Number of spin rotors	1 (3)	2 (4)	2 (6)
Number of gimbal motors	0 (0)	2 (4)	0 (0)
Number of brake coils	0 (0)	0 (0)	2 (6)
1D maneuvering time	$\sim \frac{2I_s\Delta\theta_s}{h}$	$\frac{I_s\Delta\theta_s}{2h}+\frac{2}{u}$	$\frac{I_s\Delta\theta_s}{h}$

3. Prototype Module

3.1. High-agility momentum control unit

As previously discussed, the braking mechanism is the key technology involved in enabling design compactness. In Ref-9), a "golf swing-like" braking mechanism is adopted, where an RC servo is used to immediately collide with a metal barrier that has a bolt head attached to the momentum wheel (Fig. 7a). According to uploaded YouTube videos, the latest Cubli model appears to adopt a caliper braking system using rubber, such as in a bicycle brake. In Ref-12), a rubber belt controlled by a servo motor is used to rapidly decelerate the flywheel to create an impulse of torque (Fig. 7b). Both of these methods use servo motors, which limit their compactness because of the space requirements for each outside-mounted wheel.

We thus decided to focus our efforts on an electromagnetic (E-M) braking system and not a mechanical servo. Fig. 8 illustrates the plot of mass versus brake torque for existing small E-M brakes identified from the Web. The brake torque per mass is maximal at 15 m Nm/g. In Fig. 8, the products lying in the shaded area are too heavy to jump up elegantly in a Cubli-like manner. As far as we could determine, there are no suitable brakes in the current product lineup weighing less than 100 g. Hence, it was necessary to design and develop an optimized brake coil with a miniaturized control moment unit, and Table 2 shows the specifications of our newly-developed E-M coil, which achieved a 25 m Nm/g torque density.

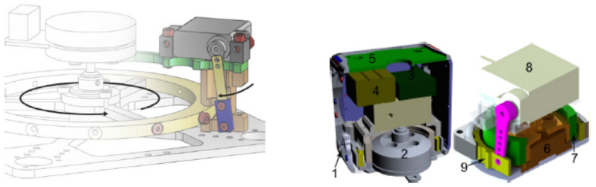

(a) (b)

Fig. 7. Figures obtained from Refs-9, 12): (a) mechanism for speedily colliding a metal bar with the side of the wheel; (b) mechanism for tightening a rubber belt. Both mechanisms utilize a servo motor.

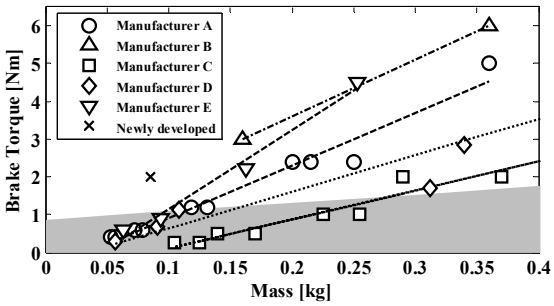

Fig. 8. Mass versus brake torque for existing E-M brakes and newly developed brake. Products in the shaded area is too heavy to wake-up its body in a Cubli-like manner.

Table 2. Developed E-M brake coil specifications (without rotor mass).

Rated voltage	DC 8.0 V
Outer diameter	ϕ70 mm
Height	12 mm
Weight (including lead wire)	84 g
Brake torque (static)	2.1 Nm
Release time	8 ms

Our proposed compact brake mechanism is illustrated in Fig. 9, which shows configuration of the E-M-based wheel braking unit. One of the reasons for the heaviness of the E-M brake is the separation between the rotating mass and the armature coil. Hence, the existing armature was eliminated by constructing the rotor wheel out of a ferromagnetic material (SUS400 series). Since the inertial moment is proportional to r^4 (r is the radius of rotating mass), the inertial moment was increased by filling the inside of the E-M brake and by maintaining an outer rotor mass at the maximum possible thickness. The leaf spring, which is normally placed on the armature side, is placed on the E-M coil side. As seen in Fig. 10, the clearance between the wheel and the E-M coil is maintained at 0.15 mm. When the brake is engaged, the coil side is attracted to the wheel side, and thus this mechanism realized the desired compactness and flatness of a braking system with dimensions of 28 mm $\times$ 100 mm $\times$ 100 mm and a mass of 345 g per unit. The moment of

inertia (MOI) of the wheel, I_w, is 1.9×10^{-4} kg m^2, which is 23.1% MOI of the ideally filled mass. Fig. 11 illustrates wheel speed versus braking time to a complete stop; the braking system has a complete stop time of less than 100 ms.

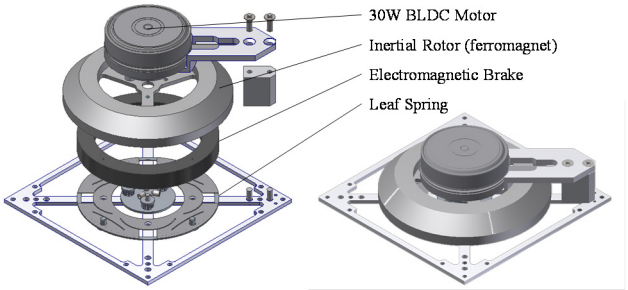

(a) (b)

Fig. 9. Configuration of E-M based on our wheel braking unit: (a) components, (b) as assembled.

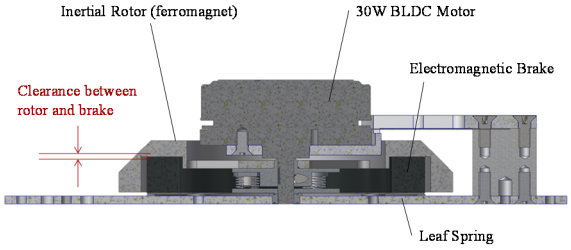

Fig. 10. Cross-sectional view of our E-M-based wheel braking unit.

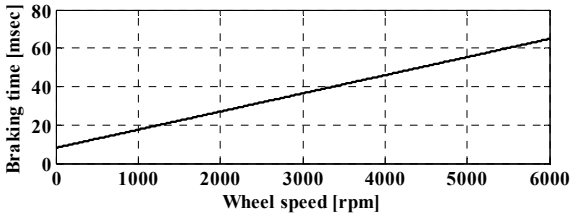

Fig. 11. Wheel speed versus braking time.

3.2. 3-axis assembly module prototype

Using small precision electronic devices that are available for commercial use, such as MEMS IMU and programmable system on-chips, was beneficial in manufacturing a prototype of our module and demonstrating its innovative concept. Figure 12 shows the 1U-sized AC all-in-one module prototype; its main specifications are shown in Table 3. The PSoC® 5LP is selected as it houses a 32-bit ARM® Cortex-M3 clocked at 80 MHz as the main controller. The IMU (MPU6050 from InvenSense Inc.) comprises a 3-axis accelerometer and a 3-axis rate-gyro. The six IMUs mounted on the housing body are connected to the main controller using three I2C buses. A 30 W brushless DC motor, the EC-45-flat (#200142) from Maxon Motor AG, drives the momentum wheels, and the embedded hall sensors of the motor are used for wheel speed sensing. The motor is controlled using a motor controller (the ESCON Module 50/5 from Maxon Motor AG). The PWM control is used for communication between the motor controller and the main computer. A wireless communications module (the XBee WiFi® (S6B)), which is of the PCB antenna type, is also built in to command the AC mode and to receive telemetry from a commercially available Android-based mobile via a WiFi router. A self-power supply consisting of two sets of lithium polymer battery packs, HP-LG335-0500- 2S-UMX (28 g × 2) from Hyperion Europe, is also included.

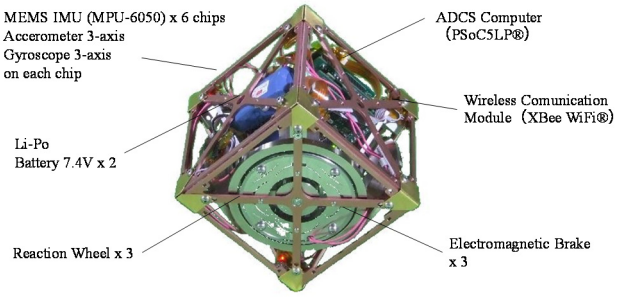

Fig. 12. A 1U-sized, miniaturized AC all-in-one module prototype.

Table 3. Specifications for the AC all-in-one module prototype.

Size	10 cm × 10 cm × 10 cm
Weight	1.38 kg (including self-batteries)
Torque scale factor	25.5 m Nm/A
Wheel MOI	1.9×10^{-4} kg m^2

In Fig. 13, the wheel of our prototype module is compared with wheels of nanosatellites from several companies in terms of volume, mass per 1-axis, storage angular momentum, and generated torque. The generated current for the wheels of some of the companies is set to 1 A, as the specification of the generated current is unknown. It is evident that our prototype is sufficiently competitive in terms of volume and weight, even though other devices such as the gyros and the processing computer, are included in the mass. However, the disadvantage of our product lies in the momentum storage, which is caused by the wheel material selected. Therefore, it will be necessary to adopt another ferromagnetic material of higher density to strengthen the momentum storage of our prototype.

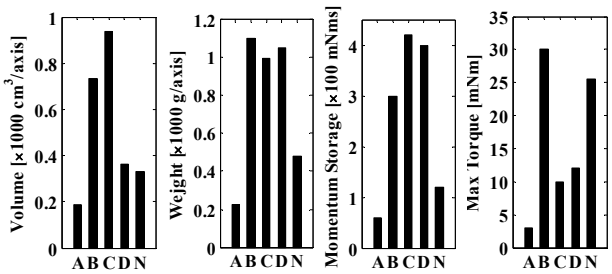

Fig. 13. Benchmark study. A: RW-0.060-28 (Sinclair Interplanetary), B: TA6494 (Tamagawa Seiki Co., Ltd.), C: 05020-ASY (Surrey Satellite Technology Ltd.), D: Higher Momentum Micro Wheel (Mitsubishi Precision Co. Ltd.), and N: Proto-type module. Mass of N includes all devices, other than wheels.

4. Experimental Results

4.1. Self-balancing test

To demonstrate that the assembled module has the necessary attitude-sensing and actuator functions, we examine its self-balancing control on an edge and corner. The sensing method is based on that in Ref-13) and the controlling method in Ref-14). On each axis, a 0.05° (3σ) tilt angle accuracy is achieved (as shown in Fig. 14).

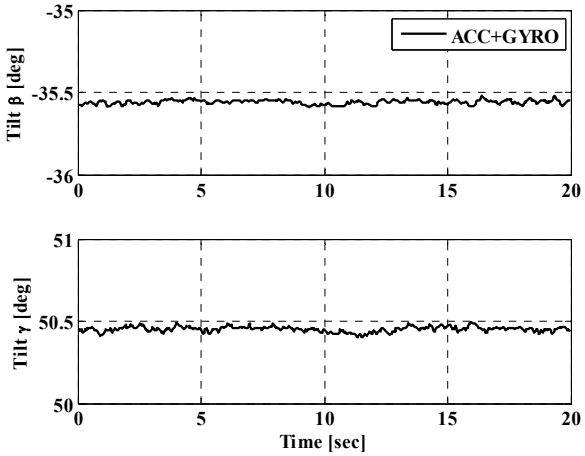

Fig. 14. Tilt angle accuracy. β and γ are tilt angles of gravity vector[13].

4.2. Rapid moment exchange function test

To confirm braking functionality, an attractive jumping test is examined[9,14]. Figure 15a shows the jumping sequence for the cube edge using an X-side brake, and Fig. 15b shows the jumping sequence for the corner using the Y- and Z-side brakes. In addition, Fig. 16 shows the change in tilt angle measured by the on-board IMU sensors. Each jump was performed five times, and the attitude change of the cube (within 1 s) can be repeatable successively.

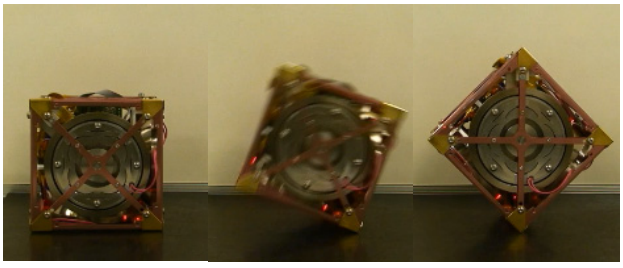

(a) t = 1.00 s, t = 1.13 s, t = 1.47 s

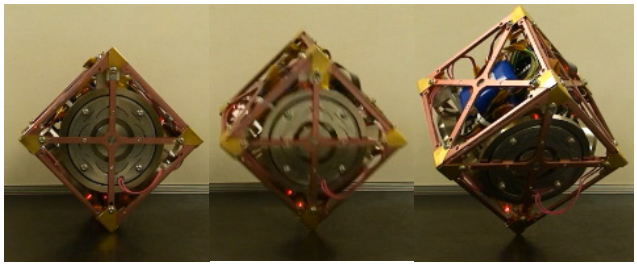

(b) t = 1.00 s, t = 1.07 s, t = 1.74 s

Fig. 15. Snapshots of high-agility maneuvering demonstrations: a) Sequence of jumps along cube edge; b) Sequence of jumps along cube corner.

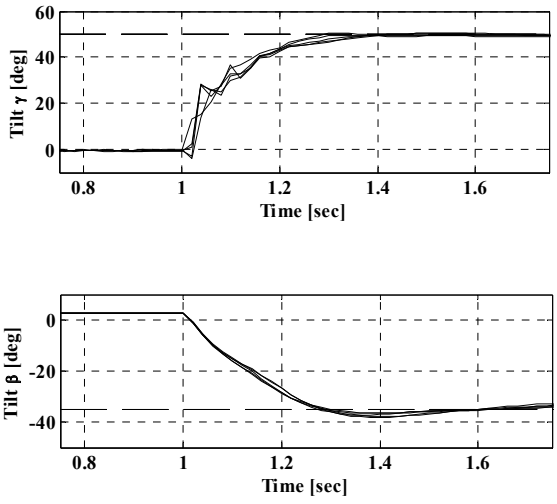

Fig. 16. Jumping performance repeatability (5 replicates): a) Sequence of jumps along cube edge; b) Sequence of jumps along cube corner.

Finally, the 1D maneuver concept demonstration is conducted; Fig. 17 shows the 1D maneuver configuration with two wheels (see Fig. 4a) on an air floating table, where the MOI of the table is about 0.4 kg m^2. The two units of the wheel are arranged coaxially, and are then rotated at the same speed but in reverse directions. The lower wheel is then stopped at the maneuver starting time and the air floating table begins to rotate. After 5 s, the upper wheel is stopped. Figure 18 shows results of the table rotation rate around the Z-axis, and the 2-wheel rotation speed, where a high speed average rotation rate of 16.7 deg/s is obtained, with a large attitude change of 83.5° at 5 s. The 1D demonstration shows that a rest-to-rest maneuver can be realized with our proposed concept.

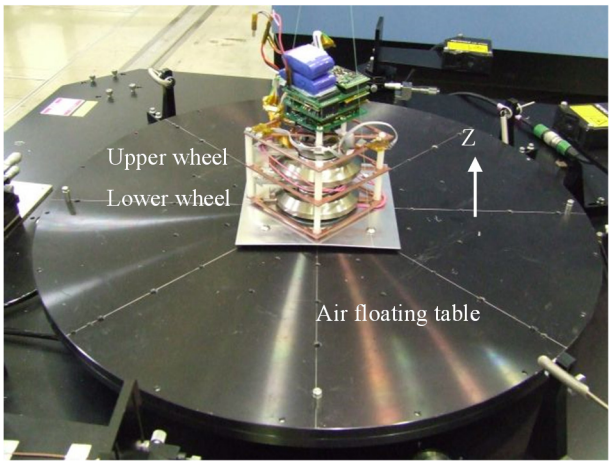

Fig. 17. Configuration of 1-dimension maneuver demonstration.

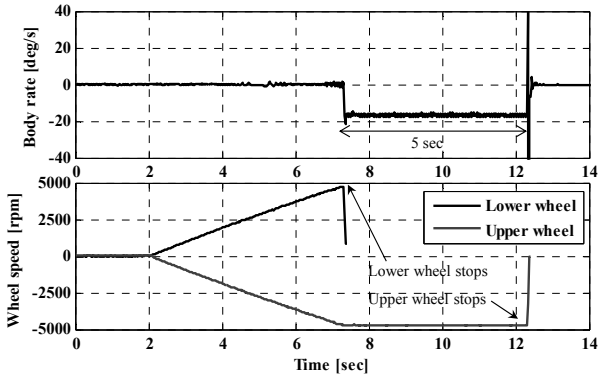

Fig. 18. Result of 1-dimension maneuver demonstration.

5. Conclusions

In this study, a three-axis attitude control function module was assembled into a highly integrated cubic package 10^3 cm^3 dimension (1U-sized). The key feature of the cubic module is its high-agility functionality, which is realized by a novel, compact electromagnetic braking mechanism combined with a ferromagnetic wheel. Our proposed concept was compared with existing 1-axis wheel assemblies and the conventional CMG scheme in terms of momentum storage per mass/volume, maneuvering speed, and compactness. The all-in-module was found to have particular merit in terms of space saving. The maneuvering time of our proposed method was determined to be faster than that of the conventional CMG scheme, if the maneuver angle was below the threshold angle (which is larger if the satellite moment of inertia is smaller). A prototype of the all-in-one module was manufactured to demonstrate our innovative concept. The self-control function worked with 0.05° accuracy, and a jump test using rapid moment exchange function was performed five times, showing that the attitude change of the cube within 1 s can be repeated successively. Finally, a 1D maneuver concept demonstration was conducted; this showed that a rest-to-rest maneuver can be realized using our proposed concept.

Acknowledgments

This study was conducted under JAXA's competitive innovation research program in FY2014. The authors gratefully acknowledge Miki Pulley Co., Ltd. and Ono Denki Co., Ltd. for supporting a part of this study.

References

1) ISIS initiative, CubeSatShop.com–Attitude Control Systems, http://www.cubesatshop.com/.
2) Bowen, J., Tsuda, A., Abel, J. and Villa, M.: CubeSat Proximity Operations Demonstration (CPOD) Mission Update, *2015 IEEE Aerospace Conference, Montana*, 2015.
3) Lappas, V., Micro CMGs for Agile Small Satellites: Design and In-orbit Tests, *Proceedings of the 6th International ESA Conference on Guidance, Navigation and Control Systems*, Loutraki, Greece, 2005.
4) Hao, T., Matunaga, S.: Singular Steering Logic Analysis using Control Moment Gyros for Nanosatellite TSUBAME, *Proceedings of the 64th International Astronautical Congress, Beijing, China*, 2013
5) Vasquez, R. A.: Wearable CMG Design for the Variable Vector Countermeasure Suit, *2015 IEEE Aerospace Conference, Montana*, 2015.
6) Yoshimitsu, T., Kubota, T., Nakatani, I., Adachi, T., and Saito. H.: Microhopping robot for asteroid exploration. *Acta Astronautica*, 52(2-6):441–446, January 2003.
7) Dietze, C., Herrmann, S., Kuß, F., Lange, C., Scharringhausen, M., Witte, L., van Zoest, T., and Yano H.: Landing and mobility concept for the small asteroid lander MASCOT on asteroid 1999 JU3. *In 61st International Astronautical Congress*, 2010.
8) Reid, R. G., Roveda, L., Nesnas, I. A. D., and Pavone, M.: Contact Dynamics of Internally-Actuated Platforms for the Exploration of Small Solar System Bodies, *International Symposium on Artificial Intelligence, Robotics and Automation in Space*, 2014.
9) Gajamohan, M., Mertz, M., Thommen, I., and D'Andrea, R.: The Cubli: A Cube that can Jump Up and Balance, *2012 IEEE/RSJ International Conference on Intelligent Robots and Systems*, Vilamoura, Algarve, Portugal, 2012, pp. 3722-3727.
10) Greenbaum, A., Brady, T., Dennehy, C., and et al.: Understanding International GNC Hardware Trends, *IEEE Aerospace Conference, Montana*, 2015.
11) Yatsu, Y., Ito, K., Kurita, S., and et. al.: Pre-flight performance of a microsatellite TSUBAME for X-ray polarimetry of gamma-ray bursts, *Proceedings of SPIE, Space Telescopes and Instrumentation 2014: Ultraviolet to Gamma Ray*, **9144**, Montreal, Canada, 2014.
12) Romanishin, J. W., Gilpin, K., and Rus D.: M-Blocks: Momentum-driven, Magnetic Modular Robots, *2013 IEEE/RSJ International Conference on Intelligent Robots and Systems*, Tokyo, Japan, 2013, pp. 4288-4295.
13) Trimpe, S. and D'Andrea, R.: Accelerometer-based Tilt Estimation of a Rigid Body with only Rotational Degrees of Freedom, *2010 IEEE International Conference on Robotics and Automation*, Anchorage, Alaska, USA, 2010.
14) Gajamohan, M., Muehlebach, M., Widmer T., and D'Andrea, R.: The Cubli: A Reaction Wheel Based 3D Inverted Pendulum, *2013 European Control Conference*, Zürich, Switzerland, 2013.